RF Energy Harvesting by D2D Nodes within a Stochastic Field of Base Stations via Mobility Diversity

S. Kusaladharma[1], C. Tellambura[1], *Fellow*, *IEEE*, and Z. Zhang[2]
[1]Department of Electrical and Computer Engineering, University of Alberta, Canada
[2]Wireless Technology Cooperation Department, Huawei Technologies Co., Ltd, Shanghai, 201206, P.R.C.
Email: kusaladh@ualberta.ca, zhangzhang4@huawei.com and ct4@ualberta.ca.

Abstract—Device-to-device (D2D) where users communicate directly with each other with limited base station involvement can significantly improve spectral efficiency, energy efficiency, and throughput in future cellular networks. Moreover, RF (radio frequency) energy harvesting (EH) promises to prolong the battery life and improve energy efficiency of D2D communication. Mobility diversity refers to the gains accrued via user mobility. Is it possible to exploit the mobility of D2D terminals via user movements to enhance their ability to harvest RF energy? To this end, we analyze the performance of a mobile D2D device powered by EH from the transmissions of underlying cellular base stations (BSs), whose locations are modeled as a homogeneous Poisson point process. We model the movements of D2D nodes via a modified random waypoint model. Log-distance path loss is considered, and it is assumed that EH takes place solely within harvesting zones surrounding each BS and that each D2D user requires a fixed number of charging time slots before being able to transmit. We derive the probability of a D2D device being within an EH region surrounding BSs after multiple transitions, and the probability of being within the the fully charged state using a Markov-chain approach taking into account temporal effects. It is shown that the number of transitions required to be within a harvesting region increases significantly when the harvesting threshold power increases.

Index Terms—Energy harvesting, user mobility, mobility diversity, Stochastic geometry

I. INTRODUCTION

Radio frequency (RF) energy harvesting (EH) for low powered wireless devices is an exciting preposition to improve the overall energy efficiency and to reduce the carbon footprint [1]. Thus, EH is increasingly seen as a viable technology for the future fifth generation (5G) networks [2]. RF EH can be suitable over other renewable sources such as solar or wind energy because it is less likely to be affected by weather events [3]. While RF EH can be based on either dedicated energy transmitters or ambient RF sources, the latter offers cost savings and a potentially self-sustaining nature. The development RF energy harvesting circuits has significantly progressed recently [3], [4].

However, EH from ambient sources such as cellular networks is subject to inherent uncertainty [5]. It emanates from random propagation effects (e.g., fading), heterogeneous transmit power levels, interference, and random locations of nodes. Traditionally, these impairments (especially multipath fading) have been considered as impediments to wireless communication. However, the modern viewpoint is that multipath fading can be harnessed to optimize wireless capacity and

gains. Analogously, mobility diversity refers to the exploitation of user movements to combat small-scale fading [6].

EH is especially attractive for device-to-device (D2D) communications which have been proposed for future wireless networks [7], [8]. D2D networks allow direct communication between nearby devices with limited base station involvement or supervision [9], [10]. This allows significant resource savings to the network in terms of spectral resources, processing, and energy. D2D communication is especially attractive for traffic offloading, sensor networks, and emergency communication networks .

It is also worth noting that some D2D devices are hand held or body mounted (i.e. motion enabled) [11]. Thus, in [12], the authors exploit the mobility diversity principle to maximize the net amount of energy by a mobile device. This paper is the first one to exploit the mobility diversity principle to optimize energy harvesting from an RF signal. The authors develop a motion control law for the device to maximize its net energy gain. However, in this paper, we focus on hand held D2D devices subject to human motion, and we investigate the effect of this mobility to harvest energy. Note that we do not assume that EH output is the sole power source of a transmitting node, rather a complementary one.

A. Prior Research

EH performance of sensor and D2D nodes has been intensively researched. For example, [4] proposes a novel network model and uses stochastic geometry to analyze EH devices co-existing with a primary network, while [13] extends this model by incorporating path loss inversion based power control and incomplete power depletions. Meanwhile references [5], [7] develop EH protocols when D2D devices harvest energy from a multi-channel cellular network. Moreover, [14] characterizes network performance when relay devices harvest energy, and analytically model the amount of the harvested energy incorporating temporal effects via Markov chains. An energy field model is introduced in [15] to analyze the coverage probability of a network powered by ambient energy harvesting. The authors of [12] incorporate user mobility in characterizing the energy harvesting performance, and show that mobility diversity can indeed improve the efficacy of EH process. In [16], an analytical model is proposed for energy harvesting via the ambient cellular network and power beacons under

multi-channel conditions using stochastic geometry, while [17] characterizes the performance of D2D energy harvesting in terms of the sum rate without degrading the quality-of-service experience by regular cellular users. Furthermore, a novel cellular architecture is proposed within [18] which integrates energy harvesting and social-aware networking for D2D communications, and it is shown that significant spectral and energy gains are achievable.

B. Motivation and Contribution

Despite extensive EH research, as far as we know only [12] has improved the EH performance by exploiting mobility diversity. However, [12] considers EH mobile devices with a single transmitting BS which acts as a dedicated power source. However, in this paper, we consider the spatial randomness of random number of BSs. Specifically, the locations of the BSs are modeled as a point process. The motion of D2D nodes is modeled via the random way point model [19].

To this end, we consider a random set of cellular BSs in $\mathbb{R}^2$ modelled stochastically as a Poisson point process (PPP). The transmit signals of these BSs are subject to fading and log-distance path loss. The EH devices can harvest energy as long as they are within specific harvesting zones around the BSs where the received ambient RF power is greater than the threshold power level required for their conversion circuits to operate. Whenever a device is outside of a harvesting region and requires to cinduct a transmission, it conducts a motion (i.e. the user carrying the EH device moves after receiving a notification) till it is within the harvesting region. Our specific contributions are summarized below.

1) We propose an EH protocol for motion enabled D2D devices which have no prior knowledge of base station locations.
2) Using tools from stochastic geometry, we derive the probability of a random D2D node being inside a harvesting region surrounding a base station at any given time.
3) When an energy harvesting D2D user requires multiple harvesting time slots, we derive the steady state transmission probability of such a device using a Markov chain based approach taking into account temporal correlations.

This paper is organized as follows. Section II introduces the system model in terms of the spatial distribution of nodes, signal and channel characteristics, and energy harvesting protocol. Subsequently, Section III derives the steady state transmission probability of a typical energy harvesting device while Section IV evaluates the probability of the energy harvesting device being within the harvesting region. Section V illustrates numerical results while Section VI concludes the paper.

Notations: $\Pr[A]$ is the probability of event A, $f_X(\cdot)$ is the probability density function (PDF), $F_X(\cdot)$ is the cumulative distribution function (CDF), $M_X(\cdot)$ is the MGF, and $\mathbb{E}[\cdot]$ denotes the expectation.

Name	PDF
Φ_{cb}	Process of BSs
λ_{cb}	BS density
Φ_{cu}	Process of cellular users
λ_{cu}	Cellular user density
Φ_{eh}	Process of EH D2D devices
λ_{eh}	D2D user density
P	Transmit power of a BS
α	Path loss exponent
P_γ	Threshold power level for an energy harvest
T	Time slot length
N	Number of charging time slots required to fully charge
$\mathcal{D}_t$	A typical EH device
r_j	Threshold distance between $\mathcal{D}_t$ and the j-th BS to harvest energy
$\mathcal{H}$	Harvesting region
v	Velocity of $\mathcal{D}_t$ during motion
θ	Angle of $\mathcal{D}_t$ during motion
p_{st}	Steady state transmission probability of $\mathcal{D}_t$
p_c	Probability of $\mathcal{D}_t$ being fully charged
ν	Probability that $\mathcal{D}_t$ has data to transmit
Q	State transition matrix
q	Probability of transition between state 0 and 1
q_i	Probability of $\mathcal{D}_t$ being within the harvesting region before the $i+1$-th time slot
ω_k	Steady state probability of being within the k-th state
W	Average number of transitions required

TABLE I: List of used symbols.

II. SYSTEM MODEL

A. Spatial Model

We consider a system where EH nodes are co-located with an overlaying cellular network spanning $\mathbb{R}^2$. The cellular network is composed of BSs and user devices which are located randomly (Fig. 1). While the locations of BSs are traditionally pre-planned, the advent of small cells, femto access points, and heterogeneous networks have made modern wireless networks inherently random. On the other hand, the locations of cellular users and energy harvesting devices are always random. Therefore, mathematical approaches such as stochastic geometry must be used to model these networks. Therefore, we will model the cellular BSs using homogeneous PPPs [20]. The PPP can accurately model even pre-planned wireless networks while allowing tractable analysis, which has made it popular among researchers. In a homogeneous PPP with node density per unit area λ, the probability of having k nodes within a given area $\mathcal{A}$ is given by [20]

$$\Pr[N(\mathcal{A}) = k] = \frac{(\lambda \mathcal{A})^k}{k!} e^{-\lambda \mathcal{A}}. \qquad (1)$$

Let the PPP of cellular BSs be Φ_{cb} with a density of λ_{cb}. It should noted that because homogeneous PPPs are used, λ_{cb} is constant over all $\mathbb{R}^2$. Similarly, let the cellular receivers form
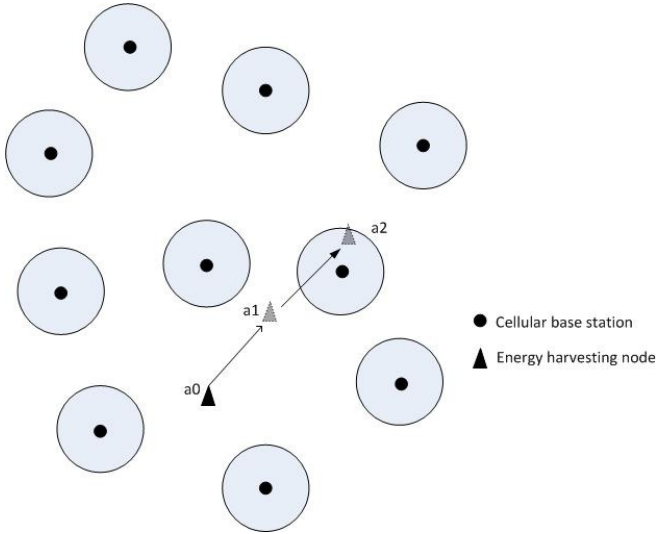
Fig. 1: System model. The shaded regions represent the harvesting zones. The EH node initially located at a_0 moves; first to a_1 and subsequently to a_2. As a_2 is within the harvesting zone, it concludes its motion there. Only a single EH node is shown for clarity. While not shown in the figure, it should be noted that harvesting zones could partially overlap.

a PPP of Φ_{cu} with density λ_{cu}. The energy harvesting nodes also form their own PPP Φ_{eh} with density λ_{eh}.

In the cellular system, the users connect with their closest base station. Thus, the BSs form Voronoi cells. We assume without the loss of generality that $\lambda_{cu} >> \lambda_{cb}$, and that all cellular BSs are fully loaded (i.e. active). However, partial loading cases can be easily incorporated by thinning the PPP of cellular BSs as necessary. For example, if only a κ fraction of BSs are active, the active BSs form a thinned homogeneous PPP with density $\kappa \lambda_{cb}$ [5].

B. Signal Model

In this work, we will assume full frequency reuse and each BS serves only a single user. However, the case of multiple users per BS can be easily incorporated [5]. Each cellular BS transmits at power P. While power control procedures are pervasive in modern cellular [21], power control is left open as a future research topic.

We consider Rayleigh fading and log-distance path loss. With Rayleigh fading, the channel power gain $|h|^2$ has the probability distribution $f_{|h|^2}(x) = e^{-x}, 0 \leq x \leq \infty$. The fading gains are assumed to be independent between different pairs of users. With log-distance path loss, the received power $P_R = Pr^{-\alpha}$ where P is transmit power, r is distance and α is the path-loss exponent.

C. Network Operation

The cellular downlink is divided into time slots of duration T each. It should be noted that these time slots can refer to frames or super frames without the loss of generality. We further assume that all cellular BSs are fully synchronized, and

that the EH nodes also synchronize with the cellular network for the purposes of EH. These are standard assumptions.

In this paper, we only consider EH through ambient RF energy from the cellular base stations, and ignore other backup power sources. Moreover, due to practical requirements of the energy harvesting circuitry, we assume that the ambient received power must be greater than a certain threshold (P_γ) for the feasibility of EH. If $\mathcal{D}_t$ is a typical EH node located at x, and the location of a cellular BS is y_j where $y_j \in \Phi_{cb}$, the distance between $\mathcal{D}_t$ and the j-th cellular BS is written as $\hat{r}_j = ||x - y_j||$. Formally, the node can thus harvest energy from the j-th cellular BS whenever $P\hat{r}_j^{-\alpha} > P_\gamma$. It should be noted that the effect of small-scale fading has been omitted because it averages to 1 within a specific time slot. Thus, for the purposes of this paper, the channel coherence time is significantly lower than T. For $\mathcal{D}_t$ to harvest sufficient energy from the j-th cellular BS, it should be within a distance of $r_j = \left(\frac{P}{P_\gamma} \right)^{\frac{1}{\alpha}}$ from it. Generalizing this concept, for $\mathcal{D}_t$ to harvest energy from any cellular base station, it has to be within a harvesting region $\mathcal{H}$ where $\mathcal{H} = \bigcup_{j \in \Phi_{cb}} b(y_j, r_j)$. Here $b(y_j, r_j) \in \mathbb{R}^2$ denotes a disc shaped area of radius r_j surrounding y_j. While more realistic EH regions based on the aggregate ambient energy can also be considered, they are more complicated, and we defer such analysis for future work. Furthermore, for mathematical tractability, independent of the location and capability to harvest energy from multiple BSs, node $\mathcal{D}_t$ harvests a fixed amount of energy at a time slot when it is inside the harvesting region $\mathcal{H}$. This assumption is popular in the literature considering zone based EH models [4].

In this paper, we assume that $\mathcal{D}_t$ needs to be within a harvesting region for N time slots in order to fully charge its batteries. Unless fully charged, no transmission occurs from $\mathcal{D}_t$. It should be noted that for $\mathcal{D}_t$ to rely on EH, the transmissions have to be sporadic in nature, and not continuous. When fully charged, $\mathcal{D}_t$ transmits during the next time slot whenever it has data to transmit. We assume that each transmission results in a full depletion of power, and that $\mathcal{D}_t$ requests to resume EH anew. Because we only focus on the EH success for brevity, we do not consider the dynamics of the transmitted signal of $\mathcal{D}_t$, which will be addressed within a future paper. Therefore, receiver or sink node selection criteria or power control schemes by $\mathcal{D}_t$ are not considered. However, incorporating these factors would be interesting research challenges for the future.

D. Motion Model

The energy harvesting nodes are assumed to be mobile (i.e. by being hand held or body mounted), while the cellular BSs are stationary. However, in the energy harvesting stages, $\mathcal{D}_t$ is assumed to be static as long as its within a harvesting region (i.e. $\mathcal{D}_t$ notifies the user once charging is complete). To model the movements of $\mathcal{D}_t$, we will assume a modified version of the random waypoint model [19]. The specific protocol is described below. It should be noted that when we refer to
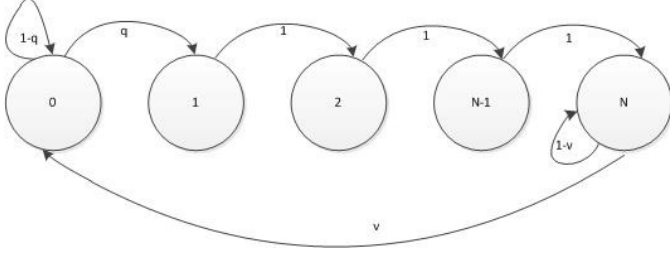
Fig. 2: Markov chain model – 0 represents the depleted state and N, the fully charged state.

the movement or stationarity of $\mathcal{D}_t$, we imply the person that holds $\mathcal{D}_t$ or the user on which $\mathcal{D}_t$ is mounted.

- When $\mathcal{D}_t$ has depleted it's power after a previous transmission, it checks whether its location x is within the harvesting region $\mathcal{H}$.
- If $x \in \mathcal{H}$, energy is harvested for N time slots. $\mathcal{D}_t$ remains static till the harvesting procedure is complete after notifying the user.
- If $x \notin \mathcal{H}$, $\mathcal{D}_t$ notifies the user, and travels for 1 time slot at any random direction θ with velocity v. Here, we assume that the EH devices are not specifically aware of BS locations. If x_1 is the location of $\mathcal{D}_t$ afterwards, it checks whether $x_1 \in \mathcal{H}$. If yes, energy is harvested for N time slots. If not, $\mathcal{D}_t$ travels in the same angle θ at velocity v for another time slot. This process continues till $\mathcal{D}_t$ is within the harvesting region.
- After the harvesting is complete, $\mathcal{D}_t$ can either remain stationary or move about either randomly or depending on its requirements till its transmission is complete.

III. Steady State Transmission Probability

Here we derive the steady state transmission probability of node $\mathcal{D}_t$, denoted as p_{st}. p_{st} depends on the probability that $\mathcal{D}_t$ is fully charged (p_c), and the probability that $\mathcal{D}_t$ has data to transmit (ν) when the charging process is finished. It should be noted that ν depends on the specific traffic generation and receiver association models which are beyond the scope of this paper. On the other hand, p_c depends on temporal effects, and we develop a Markov chain analysis.

Fig. 2 represents the state transition diagram for the energy harvesting process. The Markov chain has $N + 1$ levels as we assume $\mathcal{D}_t$ needs N charging slots. The state 0 represents the uncharged state while state N represents the fully charged state. The probability of transitioning from state 0 to state 1 is represented as q, which depends on the probability of being within the harvesting region, and will be analyzed in the subsequent section. As $\mathcal{D}_t$ remains static once within a harvesting region, the probability of transitioning from state k to $k + 1$ where $1 \leq k \leq N - 1$ after a subsequent time slot is 1. When $\mathcal{D}_t$ is fully charged (i. e. in state N) the transition probability is ν. The overall procedure can be represented in matrix form as follows where Q is the state transition matrix.

$$
Q = \begin{bmatrix}
1-q & q & 0 & 0 & . & 0 \\
0 & 0 & 1 & 0 & . & 0 \\
0 & 0 & 0 & 1 & . & 0 \\
. & . & . & & . & . \\
0 & 0 & 0 & 0 & . & 1 \\
\nu & 0 & 0 & . & . & 1-\nu
\end{bmatrix}.
$$

The probability of $\mathcal{D}_t$ in state N is denoted by p_c. As $\mathcal{D}_t$ can transmit only after arriving at the N-th state, p_c is critical in assessing the performance. If $\omega = [\omega_0 \; \omega_1 \; .. \; \omega_N]$ is the vector of steady state probabilities, we may express ω at steady state as

$$
\omega = Q\omega. \tag{2}
$$

Thus, similar to the derivations in [4], [5], we can solve (2) to obtain the following equations:

$$
q\omega_0 - \nu\omega_N = 0
$$
$$
-\omega_0 q + \omega_1 = 0
$$
$$
-\omega_1 + \omega_2 = 0
$$
$$
-\omega_2 + \omega_3 = 0
$$
$$
\vdots \tag{3}
$$
$$
-\omega_{N-1} + \nu\omega_N = 0. \tag{4}
$$

Using (3) and noting that $\omega_0 + \omega_1 + \cdots + \omega_N = 1$, we obtain

$$
p_c = \omega_N = \frac{q}{q + \nu + (N-1)q\nu}. \tag{5}
$$

IV. $\mathcal{D}_t$ in the Harvesting Region

We now derive the probability of $\mathcal{D}_t$ being within the harvesting region $\mathcal{H}$ (q). Without the loss of generality, let $\mathcal{D}_t$ be located initially at the origin. As per Section II, $\mathcal{D}_t$ moves during each time slot till it comes within a harvesting region. Therefore, the probability of $\mathcal{D}_t$ being within $\mathcal{H}$ after each subsequent time slot needs to be taken into account for the derivation of q. Thus, we can write

$$
q = \frac{1}{W + 1}, \tag{6}
$$

where W is the average number of required transitions. W can be written as

$$
W = \sum_{t=1}^{\infty} t q_t \prod_{s=0}^{t-1} (1 - q_s), \tag{7}
$$

where $q_i, i = 0, 1 \ldots$ is the probability that $\mathcal{D}_t$ is within $\mathcal{H}$ before the $i + 1$-th time slot, and t is the number of time slots that $\mathcal{D}_t$ conducts a motion. W is an important metric for $\mathcal{D}_t$ considering that a higher W means a larger time is spent trying to locate a harvesting region.

The probability of $\mathcal{D}_t$ being within $\mathcal{H}$ at the onset is q_0. Using the void probability of PPPs, we can obtain q_0 as the complement of having 0 cellular BSs within $b(0, r_j)$. Thus, we have

$$
q_0 = 1 - e^{-\pi\lambda_{cb}\left(\frac{P}{P_\gamma}\right)^{\frac{2}{\alpha}}}. \tag{8}
$$

Now, to find q_s for $s > 0$, we need the distribution of the distances from $\mathcal{D}_t$ to the cellular BSs. The distance r_k from the origin (the initial location of $\mathcal{D}_t$) to the k-th nearest cellular BS (denoted as $\mathcal{C}_k$) is distributed as [22]

$$f_{r_k}(x) = \frac{2(\pi\lambda_{cb})^k}{(k-1)!} x^{2k-1} e^{-\pi\lambda_{cb}x^2}, 0 < x < \infty. \quad (9)$$

Because the cellular BSs are stationary, the distance distributions will change whenever $\mathcal{D}_t$ moves at velocity v at an angle θ. Let $r_k(s)$ be the distance from $\mathcal{D}_t$ to the cellular BS which was initially the k-th closest [1] ($\mathcal{C}_k$) after moving for s time slots. Via the cosine rule, we can write

$$r_k(s) = \sqrt{r_k^2 + (vsT)^2 + 2vsTr_k\cos\theta}. \quad (10)$$

Let ρ_k be the probability that $\mathcal{C}_k$ is within a distance of r_j from $\mathcal{D}_t$ after moving for s time slots. Thus, we obtain

$$\rho_k = \Pr[r_k(s) < r_j]$$
$$= \Pr\left[r_k < \sqrt{\left(\frac{P}{P_\gamma}\right)^{\frac{2}{\alpha}} + (vsT)^2(\cos^2\theta - 1)} - vsT\cos\theta\right]$$
$$= \mathbb{E}_\theta\left[1 - \sum_{i=0}^{k-1} \frac{(\lambda_{cb}\pi U_s^2)^i}{i!} e^{-\pi\lambda_{cb}U_s^2}\right], \quad (11)$$

where U_s is given as

$$U_s = \sqrt{\left(\frac{P}{P_\gamma}\right)^{\frac{2}{\alpha}} + (vsT)^2(\cos^2\theta - 1)} - vsT\cos\theta \quad (12)$$

Even if a single BS is within r_j, $\mathcal{D}_t$ will be able to harvest energy. Therefore, we can write q_s as

$$q_s = 1 - \prod_{k=1}^{\infty}(1 - \rho_k). \quad (13)$$

After substituting the relevant terms, we can finally obtain the steady state probability of being within the fully charged state p_c as (14), where the final expression for W is given in (15).

V. Numerical Results

We now present numerical results for p_c and the average number of transitions (W). Simulation is conducted in MATLAB under $P = 1$, $T = 1$, $\nu = 0.5$, $N = 5$, and $\alpha = 3$, and the theoretical results are evaluated using Wolfram Mathematica (infinite sums quickly converged for finite t and k). Because the simulation coincides with the theoretical results, it has not been specially highlighted.

Fig. 3 plots the average number of transitions required to harvest energy with respect to the energy harvesting threshold P_γ. The average number of transitions increases steadily with P_γ for all the velocities considered, and is extremely low beyond a system-specific threshold value. This is due to the increasing radii of harvesting zones as P_γ reduces, which in turn increases the probability of being within one. However,

the higher the velocity, the lower the number of transitions required. If $\mathcal{D}_t$ is outside the EH zone $\mathcal{H}$, there is a higher probability that $\mathcal{D}_t$ is still outside $\mathcal{H}$ after a transition when v is low due to correlations.

The probability of node $\mathcal{D}_t$ being at state N at steady state (p_c) is plotted in Fig. 4 against velocity (v). While increasing the velocity slightly increases p_c, but the rate of increase also diminishes. The value at which the curves flatten out is the value if $\mathcal{D}_t$ sees a new realization of Φ_{cb} after each transition. Moreover, the effect of velocity is higher for lower BS densities; the change in p_c when $\lambda_{cb} = 0.001$ is minute. With a high density of base stations, $\mathcal{D}_t$ has a higher chance of arriving within $\mathcal{H}$ irrespective of the velocity. While the charging probability is low for the values used, a lower P_γ, a higher P, a lower α, and a higher λ_b among other factors would significantly increase the charging probability.

VI. Conclusion

This paper investigated the process of ambient cellar RF energy harvesting by a mobile D2D device. The locations of cellular BSs and path loss were modeled as a homogeneous PPP and log-distance, respectively. Furthermore, the movements of D2D devices followed the modified random waypoint model. In discrete time slots, the D2D devices were assumed to repeatedly transition to a new location until they came within a harvesting zone, and each device needs N time slots within a zone to be fully charged. Using a Markov chain based approach, the probability of the fully charged state was derived. The numerical results show that higher velocities and BS densities reduce temporal correlations, thus reducing the required time slots for transitions and increasing p_c.

References

[1] M. Peng, Y. Li, T. Quek, and C. Wang, "Device-to-device underlaid cellular networks under Rician fading channels," *IEEE Trans. Wireless Commun.*, vol. 13, no. 8, pp. 4247–4259, Aug 2014.

[2] A. Ã. Ercan, M. O. Sunay, and I. F. Akyildiz, "Rf energy harvesting and transfer for spectrum sharing cellular IoT communications in 5G systems," *IEEE Trans. Mobile Comput.*, vol. 17, no. 7, pp. 1680–1694, July 2018.

[3] R. Atat, L. Liu, N. Mastronarde, and Y. Yi, "Energy harvesting-based D2D-assisted machine-type communications," *IEEE Trans. Commun.*, vol. 65, no. 3, pp. 1289 – 1302, 2017.

[4] S. Lee, R. Zhang, and K. Huang, "Opportunistic wireless energy harvesting in cognitive radio networks," *IEEE Trans. Wireless Commun.*, vol. 12, no. 9, pp. 4788–4799, September 2013.

[5] S. Kusaladharma and C. Tellambura, "Performance characterization of spatially random energy harvesting underlay D2D networks with transmit power control," *IEEE Trans. Green Commun. and Net.*, vol. 2, no. 1, pp. 87–99, March 2018.

[6] J. Smith, M. Olivieri, A. Lackpour, and N. Hinnerschitz, "RF-mobility gain: concept, measurement campaign, and exploitation," *IEEE Wireless Communications*, vol. 16, no. 1, pp. 38–44, 2009.

[7] A. Sakr and E. Hossain, "Cognitive and energy harvesting-based D2D communication in cellular networks: Stochastic geometry modeling and analysis," *IEEE Trans. Commun.*, vol. 63, no. 5, pp. 1867–1880, May 2015.

[8] L. Pei, Z. Yang, C. Pan, W. Huang, M. Chen, M. Elkashlan, and A. Nallanathan, "Energy-efficient d2d communications underlaying NOMA-based networks with energy harvesting," *IEEE Commun. Lett.*, vol. 22, no. 5, pp. 914–917, May 2018.

---

[1] This BS may not necessarily be the k-th closest after $\mathcal{D}_t$ moves.

$$p_c = \frac{1}{1 + \frac{\nu}{\frac{1}{W+1}} + (N-1)\nu} \qquad (14)$$

$$W = \sum_{t=1}^{\infty} t \left(1 - \prod_{k=1}^{\infty} \left(1 - \mathbb{E}_\theta \left[1 - \sum_{i=0}^{k-1} \frac{\left(\lambda_{cb}\pi \left(\sqrt{\left(\frac{P}{P_\gamma}\right)^{\frac{2}{\alpha}} + (vtT)^2(\cos^2\theta - 1)} - vtT\cos\theta\right)^2\right)^i}{i!} e^{-\pi\lambda_{cb}\left(\sqrt{\left(\frac{P}{P_\gamma}\right)^{\frac{2}{\alpha}} + (vtT)^2(\cos^2\theta - 1)} - vtT\cos\theta\right)^2}\right]\right)\right)$$

$$\times\ e^{-\pi\lambda_{cb}\left(\frac{P}{P_\gamma}\right)^{\frac{2}{\alpha}}} \prod_{s=1}^{t-1} \left(\prod_{l=1}^{\infty} \left(1 - \mathbb{E}_\theta \left[1 - \sum_{i=0}^{l-1} \frac{\left(\lambda_{cb}\pi \left(\sqrt{\left(\frac{P}{P_\gamma}\right)^{\frac{2}{\alpha}} + (vsT)^2(\cos^2\theta - 1)} - vsT\cos\theta\right)^2\right)^i}{i!} e^{-\pi\lambda_{cb}\left(\sqrt{\left(\frac{P}{P_\gamma}\right)^{\frac{2}{\alpha}} + (vsT)^2(\cos^2\theta - 1)} - vsT\cos\theta\right)^2}\right]\right)\right) \qquad (15)$$
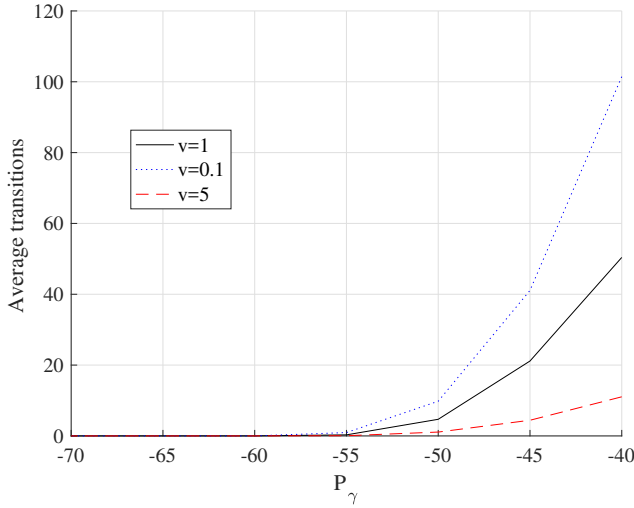
Fig. 3: The average number of transitions (W) vs. P_γ (dB) for different v. $\lambda_{cb} = 0.003$.
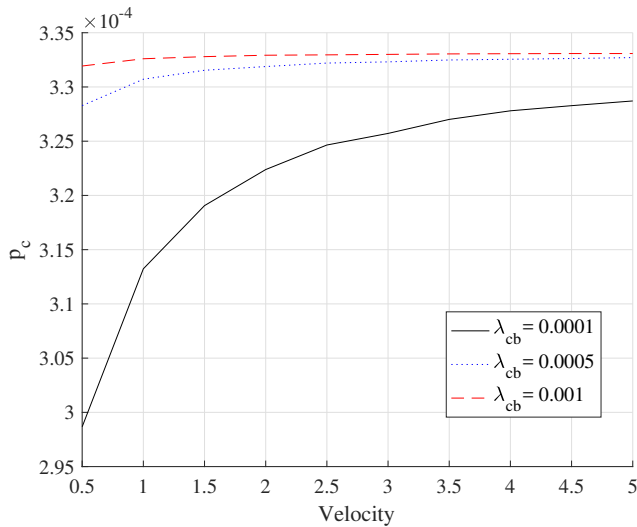
Fig. 4: p_c vs. the velocity (v) for different base station density λ_{cb} values. $P_\gamma = -50\,\text{dB}$.

[9] Y. Liu, L. Wang, S. A. R. Zaidi, M. Elkashlan, and T. Q. Duong, "Secure D2D communication in large-scale cognitive cellular networks: A wireless power transfer model," *IEEE Trans. Commun.*, vol. 64, no. 1, pp. 329–342, Jan 2016.

[10] U. Saleem, S. Jangsher, H. K. Qureshi, and S. A. Hassan, "Joint subcarrier and power allocation in the energy-harvesting-aided D2D communication," *IEEE Trans. Industrial Inf.*, vol. 14, no. 6, pp. 2608–2617, June 2018.

[11] H. Sun, Z. Zhang, R. Q. Hu, and Y. Qian, "Wearable communications in 5G: Challenges and enabling technologies," *IEEE Veh. Technol. Mag.*, vol. 13, no. 3, pp. 100–109, Sept 2018.

[12] D. B. Licea, S. A. R. Zaidi, D. McLernon, and M. Ghogho, "Improving radio energy harvesting in robots using mobility diversity," *IEEE Trans. Signal Process.*, vol. 64, no. 8, pp. 2065–2077, April 2016.

[13] S. Kusaladharma and C. Tellambura, "Energy harvesting random underlay cognitive networks with power control," in *Proc. IEEE ICC*, May 2017, pp. 1–6.

[14] H. H. Yang, J. Lee, and T. Q. S. Quek, "Heterogeneous cellular network with energy harvesting-based D2D communication," *IEEE Trans. Wireless Commun.*, vol. 15, no. 2, pp. 1406–1419, Feb 2016.

[15] K. Huang, M. Kountouris, and V. O. K. Li, "Renewable powered cellular networks: Energy field modeling and network coverage," *IEEE Trans. Wireless Commun.*, vol. 14, no. 8, pp. 4234–4247, Aug 2015.

[16] L. Shi, L. Zhao, K. Liang, and H. Chen, "Wireless energy transfer enabled D2D in underlaying cellular networks," *IEEE Trans. Veh. Technol.*, vol. 67, no. 2, pp. 1845–1849, Feb 2018.

[17] S. Gupta, R. Zhang, and L. Hanzo, "Energy harvesting aided device-to-device communication underlaying the cellular downlink," *IEEE Access*, vol. 5, pp. 7405–7413, 2017.

[18] L. Jiang, H. Tian, Z. Xing, K. Wang, K. Zhang, S. Maharjan, S. Gjessing, and Y. Zhang, "Social-aware energy harvesting device-to-device communications in 5G networks," *IEEE Wireless Commun.*, vol. 23, no. 4, pp. 20–27, August 2016.

[19] X. Lin, R. K. Ganti, P. J. Fleming, and J. G. Andrews, "Towards understanding the fundamentals of mobility in cellular networks," *IEEE Trans. Wireless Commun.*, vol. 12, no. 4, pp. 1686–1698, April 2013.

[20] J. F. Kingman, *Poisson Processes*. Oxford University Press, 1993.

[21] S. Kusaladharma, P. Herath, and C. Tellambura, "Underlay interference analysis of power control and receiver association schemes," *IEEE Trans. Veh. Technol.*, vol. 65, no. 11, pp. 8978–8991, Nov 2016.

[22] D. Moltchanov, "Distance distributions in random networks," *Ad Hoc Networks*, vol. 10, no. 6, pp. 1146–1166, 2012. [Online]. Available: http://www.sciencedirect.com/science/article/pii/S1570870512000224